Numerical Simulations of Jet Mixing Enhancement in a Round Jet Exhaust Using SJA

Liang Hong[1], Rubing Zhang[1], Zheng Liu[1]

[1] School of Energy and Power Engineering, Beihang University, Beijing, PRC

Abstract. Symmetric synthetic jet is used to stimulate a Mach number 0.9 and high temperature jet for the mixing enhancement. The movement of the piston-type synthetic jet is simulated by dynamic mesh based on URANS numerical methods. Jet flapping, streamwise vortex and geometric axis transformation are the jet mixing mechanism. However, the jet mixing enhancement effect depends on penetration area, which consists of penetration depth and spanwise. And the penetration area is determined by actuator nozzle diameter and blowing jet momentum. In addition, a 54% reduction in potential core length and maximum 45.8K decrease in potential temperature are achieved.

1. Introduction

Active flow control technology is a research hotspot in aerospace fields [1, 2]. Mixing enhancement is one of the methods of active flow control techniques. It has been widely used in aerospace. The propulsive jet plume is considered as a major source of inferred (lR) signature for military aircraft. In aero engine exhaust system, the use of the jet mixing can enhance the high temperature, high speed jet flow mixing with the surrounding ambient air, which can suppress the infrared signal [3-5] and plume noise [6-8]. Suppressing the infrared signal is the primary application of the current investigation.

The jet mixing enhancement methods can be identified as two major categories, passive flow control and active flow control technologies. The traditional passive flow control methods of the jet mixing enhancement include solid tabs [9-11], lobe nozzle [12, 13] and chevron nozzle [14-16]. These techniques can effectively alter the primary jet shear layers, but the performance of the aircraft exhaust system will decrease when this technique is in off-design conditions. The traditional passive flow control methods also have a thrust penalty on exhaust system. Nowadays more mature active flow control methods of the jet mixing enhancement include steady jet, pulsed jet and synthetic jet. These approaches are summarized in the review by Knowles and Saddington [17]. Active flow control methods are based on the use of the local energy inputting into the main flow, disturbing the jet flow shear layers, generating large-scale structure [18], which promotes jet mixing.

A periodic oscillation superimposed on a steady jet is the pulsed jet. The actuation frequency of the pulsation fall in a target range which is called optimal actuation frequency reflected by St. Raman et al.

[19] used two oscillating fluidic jets force rectangular primary jet, actuation at the first subharmonic of the preferred columnar instability mode founding that the CJs operating in-phase to generate a sinuous mode of forcing and out-of-phase to create a varicose mode. Parekh's et al. [20] experimental results showed that pulsed CJs actuating round jets were more effective in antisymmetric rather than symmetric actuation mode. Behrouzi's et al. [21] used 0.5% of primary jet flow CJs to excite subsonic jet shear layer finding that the performance of the pulsed CJs was strongly influenced by the CJs flow rate, pulse frequency, and phase.

Another time-periodic jet flow mixing enhancement active flow control method is the synthetic jet which is the main focus of this paper. Synthetic jet actuators are synthesized from the working fluid of the flow system, thus it can transfer momentum to the flow without a net mass injection while eliminating the need for an additional fluid source. Parekh et al. [22] used synthetic and pulsed jet from circular slit orifices injecting into low-speed shear layer, finding that tremendous increase in mixing by engaging the jet's flapping mode. Ritchie et al. [23] used nine coaxial synthetic jets to stimulate flow jet, finding that large-scale structures are more important in downstream and outside mixing layer and the small-scale mixing effects are strong in near field and downstream in inner mixing layer. David et al. [24] used a single synthetic jet to control axisymmetric free jet. The results showed that synthetic jet raise the primary jet's turbulent quantities to enhance mixing. From the mentioned above, the time-periodic jet has effects on jet mixing enhancement, although a thrust penalty. The main mechanism of this technology is flapping and streamwise vortex. Comparing with the steady jet, the time-periodic jet needs less or no bleeding air, but the thrust penalty for applying is still exist.

From the aforementioned, many investigations on time-periodic actuation of primary jet shear layers have been reported. However, much of the reported works have focused on low Re and low Mach number flow and the actuators they used also have a low-amplitude, others focused on jet vectoring and coaxial mixing. For aero engine application, it is important that the effectiveness of any enhancement technique will be demonstrated at high Re and Mach number values and the actuator must be "strong" enough. The investigation of using a high-amplitude synthetic jet forcing a high temperature primary jet to enhance jet mixing is seldom. So the piston-type SJA is used to actuate the high Re and high Mach number jet flow to study the mixing enhancement.

2 Numerical simulation model

2.1 *Domain Specification and Boundary Conditions and Computational Mesh*

The nozzle is a convergent nozzle with a convergent half angle of 11 °, an outlet diameter d of 30 mm with a short parallel-walled section. The diameter of the nozzle inlet is 1.25d. The entire length of the axisymmetric convergent nozzle is 1.8d. There are four normal injection SJAs which placed 0.1d downstream away from the nozzle outlet. The symmetric actuation mode is used. Adjacent twin antiphase synthetic jet can also achieve actuation frequency double. 3D physical domain is modeled and the computational domain is shown in figure.1. Piston-type SJA a, d (b, c) has the same phase and a, c 180 °out of phase from each other.

The inlet of nozzle with a total pressure of 1.7atm and a total temperature of 800K is defined as pressure inlet boundary condition，and $Re_d=4\times10^6$. The outlet of the computational domain is defined

as pressure outlet at a static pressure as 1atm. The actuator nozzle diameter d_0 is 0.11d. The actuation frequency is set to 200 Hz.

The movement of the piston-type actuator is simulated by dynamic mesh. The growth of the piston wall is based on remeshes methods of mesh deforming. The unsteady time step size is based on the piston crank angle step size and actuation frequency.

Multi-block, structured meshes are created for the axisymmetric convergent nozzle's computational domain using the ICEM code. The grids as shown in Fig. 1 near the nozzle wall have been refined using the standard wall function. In the streamwise (x) direction, the initial spacing of the nodes is set at 0.5, with the interval count as 150 for the downstream flow field of the whole nozzle. An expanding grid with an expansion factor of 1.03 in the y and z directions is used.

The numerical computations were conducted by the finite volume method developed by Patankar via the commercial computation fluid dynamics code Fluent [25]. The conservation equations for momentum and density-based continuity are solved together by the coupled algorithm.

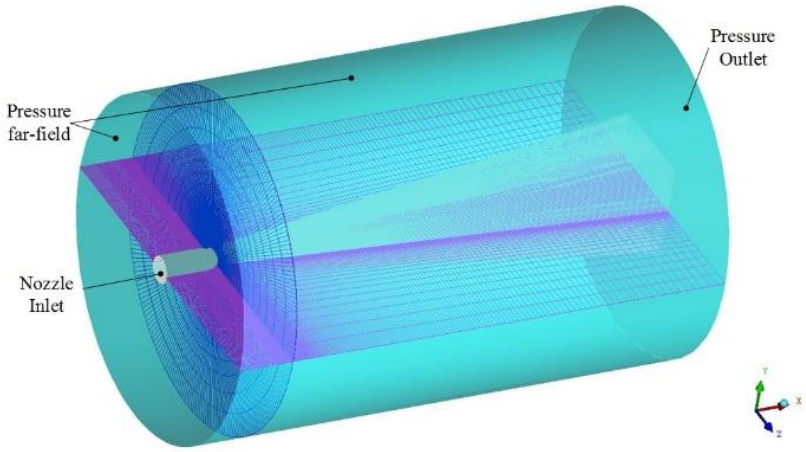

Figure 1. Computation domain boundary conditions and computational mesh

2.2 *Governing Equations and Turbulence Model*

The commercial CFD solver FLUENT with time step method is used to obtain the solution of unsteady compressible Reynolds averaged Navier-Stokes (URANS) equations in the present study. The inviscid flux vector is evaluated by second order upwind scheme with Roes flux difference splitting method. The ideal-gas model based air is set as the fluid material. The viscosity is calculated by Sutherland low, and the gravity effect can be neglected.

The turbulence model used is the RNG k-ε model. The RNG model is more responsive to the effects of rapid strain and streamlines curvature than the standard k-ε model, which explains the superior performance of the RNG model for certain classes of flows. According to the comparison between the PIV experiments of a dual synthetic jets actuator in quiescent air and numerical simulations, a RNG k-ε turbulent model [26] is most consistent with the experimental results. Therefore, the RNG k-ε turbulent model is selected for the current study.

3 Results and Discussion

3.1 *Characteristics of SJA*

Figure 2. shows the piston-type SJA which has been used in this investigation. A 19.5 mm piston within a matching cylinder with a stroke of 16.4 mm is used, such that the volume displacement is 5.5 cm^3. The cylinder cover plate with an axisymmetric orifice of diameter d_0=3.5mm. The thickness of the cylinder cover plate l is maintained l/d=2.0. The minimum clearance between the piston and the cylinder cover plate (at TDC) is 2.2 mm, yielding a maximum compression ratio of 8.45.

For the piston-type SJA, the Pr has shown a sharp increase in blowing phase, and it is even higher than the critical Pr (Pr_{cr} = 1.89, k = 1.4), thus a supersonic blowing jet exists in figure 3. That means the SJA can afford a high-momentum blowing jet.

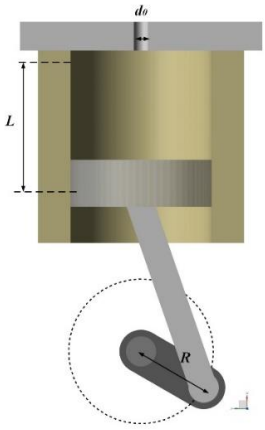

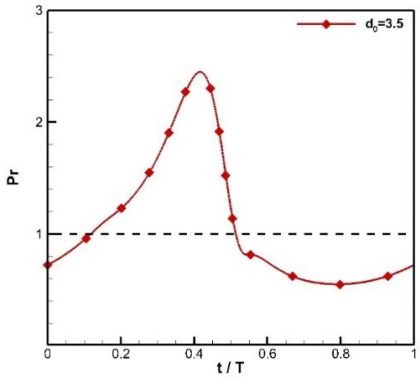

Figure 2. Schematic diagram of SJA **Figure 3.** Time-periodic Pr distributions

3.2 *Mixing enhancement mechanism analysis*

3.2.1 *Primary jet flapping.* Figure 4. shows the instantaneous and time-averaged temperature field of the actuator plane. A jet flapping happens especially at t/T=0.25 and 0.75, which can reduce the potential core length and spanwise, so it plays an important role in jet mixing. Although the symmetric actuation mode is selected, but the position of the SJA is departure from the plume jet center, thus the jet flapping phenomenon appears. However, the primary jet flaps (even not violent enough) two times with the SJA actuation frequency. It can be conclude that the jet flapping is conducive to the enhancement of the jet flow expansion and mixing between the plume jet and ambient fluid. Compared with the unforced jet flow, the size of the time-average potential core is sharp decrease. Therefore, the synthetic jet has a great effect on the jet mixing enhancement, and sag area is also appearing in this figures.

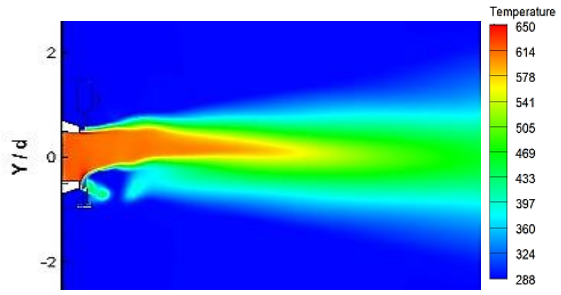

(a) t_0+1/4T

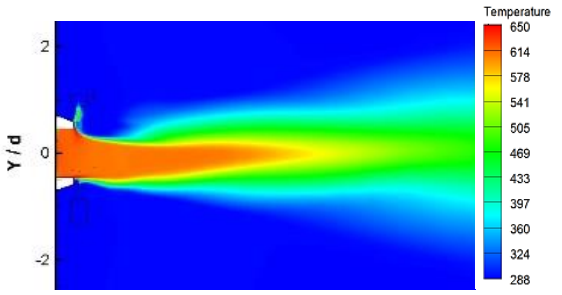

(b) t_0+3/4T

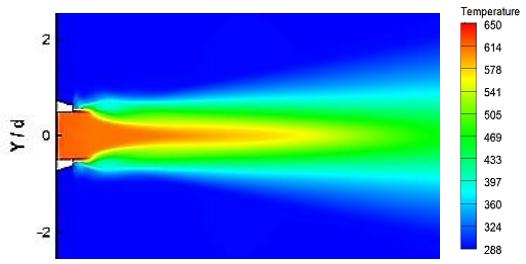

(c) time-average

Figure 4. Instantaneous temperature contours of centerline cross section of the actuation plane

3.2.2 *CVPs.* Streamwise vortices is defined as $\xi \cdot v / |v|$ [27]. And the magnitude of the streamwise vorticity has been normalized by v_e / d [28]. So, the dimensionless streamwise vorticity stv equation can be expressed as follows: $stv = \frac{d}{V_e}\left(\frac{\xi \cdot V}{|V|}\right)$. Figure 5 shows the evolution of the instantaneous stv distribution. The vorticity and position of the streamwise vortex are varying as the blowing jet momentum changes over cycle. When the synthetic jet begins to blow the primary jet, the formation of the CVPs is due to the interaction of the blowing jet and the primary jet. However, the vorticity of CVPs are not equal due to actuation of synthetic jet.

As a whole, the generation mechanism for the streamwise vortices produced by fluid actuation can be identified by two sources. The dominant source is the pressure hill formed upstream of the fluid actuation. The fluid actuation creates a pressure hill in the lateral direction, which causes the airflow to move around the fluid actuation. The result is generating a pair of streamwise vortices. The second source originates from the vortex lines shed from the sides of fluid actuation. As the jet propagates downstream, the vortex lines initially aligned parallel to the fluid actuation's side will be reoriented by the velocity gradients in the shear layer to become streamwise [28].

At 1/4T (figure 5. (c)), with blowing jet increases, the penetration depth further increases and synthetic jet blows into the primary jet, thus more ambient fluid is entrained into the primary jet, which changes the size of the potential core. The suction phase begins at 3/8T. However, the CVPs are still existing in the flow fields due to the duration of the blowing jet. At 1/2T, the CVPs disappears. And at 5/8T, the SJA repeat this process, and the evolution of the flow fields is similar to the mentioned above.

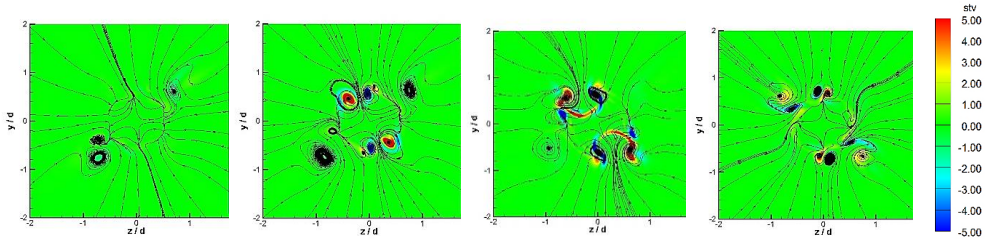

(a) t_0 (b) t_0+1/8T (c) t_0+1/4T (d) t_0+3/8T

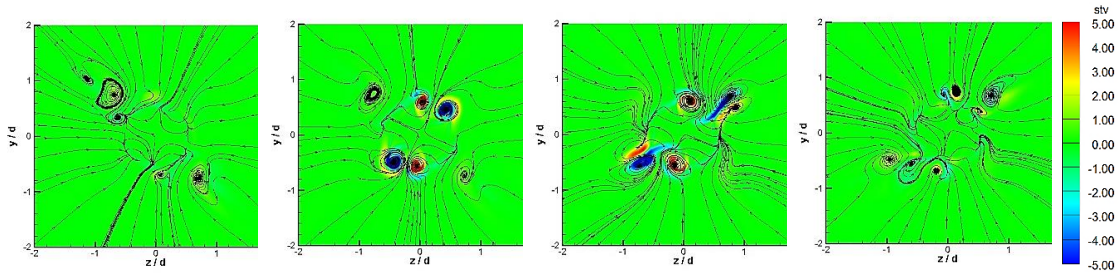

(e) t_0+1/2T (f) t_0+5/8T (g) t_0+3/4T (h) t_0+7/8T

Figure 5. Instantaneous Stv distribution at x=1.0 d.

3.2.3 *Geometric axis transformation*. The instantaneous temperature field of cross plane at x/d=1 is shown in figure 6. There is a low temperature "gap" in the potential core, due to the synthetic jet. The "gap" size increases and potential core size decreases obviously at t/T=1/4 and t/T=3/4. And the fluid of the "gap" is the ambient air, thus the temperature is low. However, the flow within the "gap" is complex, there are CVPs in this zone. As a result of this type actuation, at t=1/4T and t=3/4T, the "gap" is in the opposite direction, it can be named as geometric axis transformation. This phenomena may also promote the mixing of the ambient air and primary jet. However, the penetration area is determined by actuator nozzle diameter and blowing jet momentum.

The time-average temperature field distributions of the cross plane is show in figure 6(c). Compared with the unforced one, the size of the time-averaged potential core at cross plane is obvious decrease. And the CVPs lie in this zone, thus the CVPs play an important role in mixing enhancement.

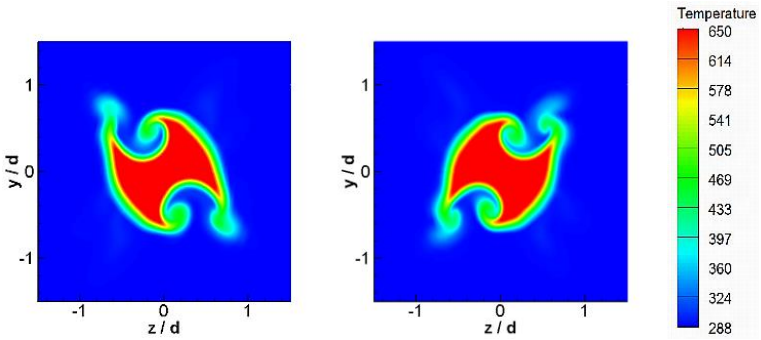

(a) t_0+1/4T (b) t_0+3/4T

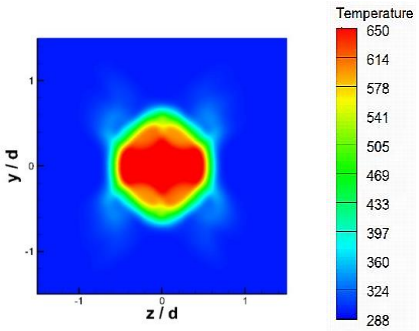

(c) time-average

Figure 6. Instantaneous temperature contours at x/d=1

3.2.4 *Evolution of 3D temperature field*. Figure 7 shows the evolution of 3D temperature field with the blowing jet at x/d=0, x/d=1, x/d=2 and x/d=3. The instantaneous temperature contour of the iso-surface is 650K. The blowing jet penetrates into primary jet at t=1/8T, changing the shape of the potential core. The moment of the blowing jet increases at t=1/4T, and the blowing jet has a strong impact on the primary jet. Compared with figure 7 (a), the sag area becomes larger and transports to the downstream, and the length of potential core becomes shorter apparently. The suction phase begins at t=3/8T. However, the preformed sag area transports alone the flow direction and the primary jet is also short. The influence of the synthetic jet on potential core is quite small at t=1/2T, and the length of potential core remains to the unforced status. After that, actuator a, d begins to blow the primary jet, and repeats this process. Compared with the unforced jet flow, the time-averaged temperature field shows that the SJA has a great effect on the jet mixing enhancement, and four sag area is seen obviously.

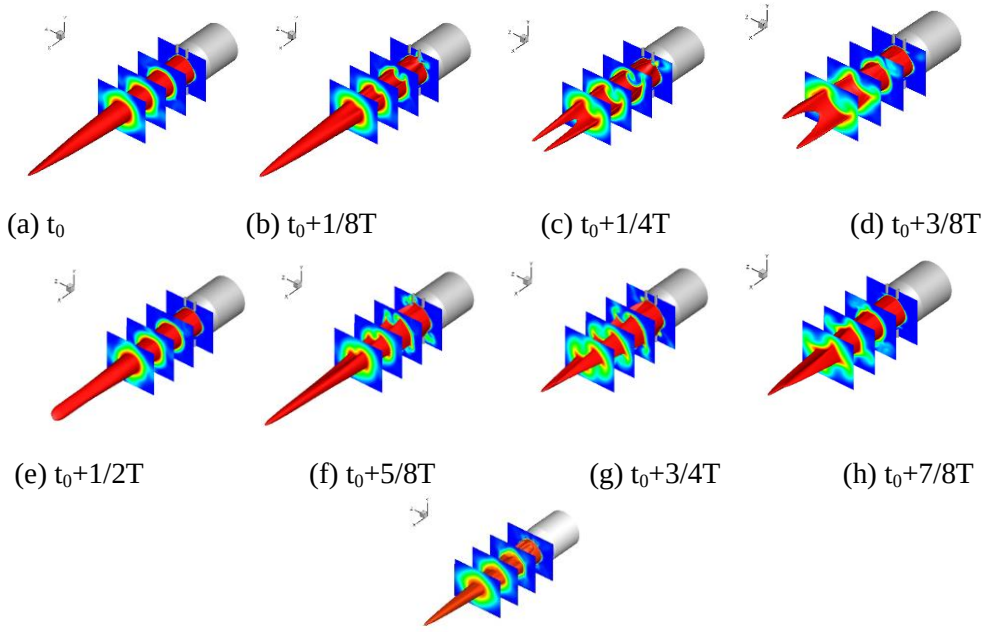

(a) t_0 (b) t_0+1/8T (c) t_0+1/4T (d) t_0+3/8T

(e) t_0+1/2T (f) t_0+5/8T (g) t_0+3/4T (h) t_0+7/8T

(i) time-averaged

Figure 7. Time sequence visualization of 3D iso-surfaces

3.2.5 *Comparison of the Jet's Centerline Temperature*. Figure 8 shows the time-averaged normalized temperature distribution of the primary flow centerline. The normalized temperature distribution of the primary jet centerline T' is used to access the mixing effectiveness. The definition of T' is as follows:

$$T' = \frac{T - T_a}{T_0 - T_a}.$$

With the SJA's actuation, the primary flow dimensionless centerline temperature decreases from x/d=2, and the length of the potential core reduces 54% and a maximum 45.8K decrease in potential core temperature. The vorticity of streamwise vortex is correlation to the penetration area, and a large penetration area can entrained more fluid into the primary flow. Thus a high-momentum and a larger nozzle diameter SJA is needed. From the analysis above, the jet flapping, CVPs and geometric axis transformation has the effects on jet mixing enhancement.

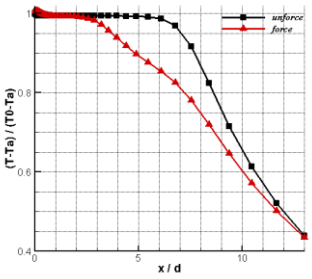

Figure 8. Comparison of the time-averaged primary jet centerline normalized temperature distributions.

4. Conclusion

Piston-type synthetic jet is used to enhance a subsonic, heat temperature jet mixing. Mixing enhancement effect is obvious. There are three main mixing mechanisms in this case, namely Jet flapping, streamwise vortex and geometric axis transformation.

Primary jet in actuator outlet plane flapping is caused by synthetic jet periodic blowing. This mechanism shortens the length of the potential core, accelerating the spread of potential core fluid to environment. CVPs plays an important role in mixing enhancement. This is due to the increase of the quality of the ambient fluid and primary jet potential core transportation, meanwhile enhancing the primary jet and environmental fluid mixing. Geometric axis transformation may promote the mixing of the ambient air and primary jet.

However, the jet mixing enhancement effect depends on penetration area. And the penetration area is determined by actuator nozzle diameter and blowing jet momentum. In addition, a 54% reduction in potential core length and maximum 45.8K decrease in potential temperature are achieved.

5. Reference

[1] Kamran M A, Manipulation of high Mach number shear layers using control jets. [D]. Loughborough Univ., U.K., 2009

[2] Edmnnd J. Field Kenneth F. Rossitto et al. Active control technology for enhanced performance operational capabilities of military aircraft, landing vehicles and sea vehicles [R].*ADA*395700. 2001. 1-1032

[3] Shripad P. Mahulikar, Hermant R. Sonawane, G. Arvind Rao. Infrared signature studies of aerospace vehicles [J]. *Progress in aerospace sciences* Vol.**43**, pp 218-245, 2007

[4] Timothy D. Smith, Alan B, Cain. Numerical simulation of Enhanced mixing in jet plumes using pulsed blowing [J]. *Journal of aircraft* Vol.**37**, No.3, 2001

[5] K Knowles, A J Saddington. A review of jet mixing enhancement for aircraft propulsion application [J]. *Journal of aerospace engineering* 2006 220:103

[6] Vinod G. Mengle. Relative clocking of enhanced mixing devices for jet noise benefit [R].*AIAA* 2005-0996

[7] Samimy M., Zaman K B M Q , and Reeder M F. Effect of tabs on the flow and noise field of an axisymmetric jets.[J] *AIAA Journal*, Vol.**31**, No.4, 1993, pp.609-619

[8] Brenton Greska, Anjaneyulu Krothapalli. High-speed jet noise reduction using microjets on a jet

engine [R]. *AIAA* 2004-2969

[9] Grettta W. J., Smith C. R., The flow structure and statics on a passing mixing tab [J]. *Fluid Eng*., ASME. Vol.**115**, pp.255-263, 1993

[10] Zaman K. B. M. Q., Reeder M F, Samimy M. Supersonic jet mixing enhancement by delta-tabs. [R] *AIAA* 1992-3548

[11] Bradbury L J S., Khadem A H. Distortion of a jet by tabs. [J] *Journal of fluid mechanics*, Vol.4, 1975, pp.801-813

[12] Mengle V. G., Dalton W. N., Lobed mixer design for noise suppression [R]. NASA contract NAS3-27394, 1998

[13] R. Malecki, W. Lord Pratt. Navier-Stokes analysis of a lobe mixer and nozzle [C]. *AIAA* 1990-0453

[14] Samimy M., Kim J H. and Clancy P S. Passive control of supersonic rectangular jets via nozzle trailing-edge modifications.[J] *AIAA Journal*, Vol.**36**, No.7,1998, pp.1230-1239

[15] Callender B., Gutmark E., Martens S., A PIV flow field investigation of chevron nozzle mechanisms [C]. *AIAA* 2004-0191.

[16] Ali Uzun,M. Yousuff Hussaini., High-fidelity numerical simulation of a chevron nozzle jet flow [C]. *AIAA* 2009-3194.

[17] K Knowles, A J Saddington. A review of jet mixing enhancement for aircraft propulsion applications [J].*Journal of aerospace engineering*, 2006 220:113

[18] Ho C M., Huerre P. Perturbed free shear layer.[J] *Annual review of fluid mechanics*, Vol.**16**, 1987, pp. 365-424

[19] Raman G, Cornelius, D. Jet mixing control using actuation from miniature oscillating jets. [J]. *AIAA Journal*, Vol.**33**, No.2, 1995, pp 365-368

[20] Parekh D E, Kibens V. Innovative jet flow control mixing enhancement experiments [R]. *AIAA* 1996-0308

[21] Behrouzi P., Mcguirk J. Flow control of tabs mixing using a pulsed fluid tab nozzle.[R]. *AIAA*. 2006-3509

[22] Parekh, V.Kibens. Innovative jet flow control mixing enhancement experiments[R].*AIAA* 1996-0308

[23] B.D.Ritchie, D.B.Mujumdar, J.M.Seitzman. Mixing in coaxial jets using synthetic actuators [J]. *AIAA* 2000-0404

[24] David A. Tamburello, Michael Amitar. Active control of a free jet using a synthetic jet[J].*International journal of heat and fluid flow* Vol.**29**, pp 967-984, 2008

[25] Patankar, S. V., Numerical heat transfer and fluid flow [J]. McGraw Hill, New York, 1980, pp.89- 109.

[26] Zhen-bing Luo, Zhi-xun Xia, Wei Luo, et al. Principle of a novel dual synthetic jets actuator based continuous flow micro-pump. [C] *AIAA* 2008-4704

[27] Bluestein H B., "Synoptic dynamic meteorology in midlatitudes," New York, Oxford Univ press, 1992.

[28] Wan, C., and Yu, S. C. M., "Numerical Investigation of the Air Tabs Technique in Jet Flow," *Journal of Propulsion and Power*, Vol. **29**, No.1, 2013.